8-13-2019

Cassava starch films reinforced with lignocellulose nanofibers from cassava bagasse

Ana P. Travalini
Ponta Grossa State University

Buddhi P. Lamsal
Iowa State University, lamsal@iastate.edu

Washington L. Esteves Magalhaes
Centro Nacional de Pesquisa de Florestas

Ivo M. Demiate
Ponta Grossa State University

Cassava starch films reinforced with lignocellulose nanofibers from cassava bagasse

Abstract
Cassava bagasse, a high-fiber coproduct of cassava starch processing, was used to produce lignocellulose nanofibers (LCNF) to apply as reinforcement in cassava starch films. LCNF-reinforced cast starch films were evaluated for changes in structural, thermal and mechanical properties and compared with control films reinforced with commercial grade nanoclay (Nclay). Five different types of cassava starch cast-films were produced: no-reinforcement control, two LCNF-reinforced, and two Nclay-reinforced, each at 0.65 and 1.3% w w−1. The LCNF morphology showed the characteristic microscopic structure of lignocellulose nanofibers, with an aspect ratio > 85 and average diameter of 4.5 nm. All reinforced films were transparent and had a good distribution of the nanoparticles within. The opacity values reduced for the films with all nanoreinforcements, compared to control. The permeability to water vapor reduced with reinforcements, with lower values for the films tested with LCNF 0.65 and Nclay 1.3. Thermal stability improved with 1.3% of LCNF and both concentrations of Nclay. Tensile stress for films increased and elongation at break value decreased with both types of nanoreinforcements.

Keywords
Starch, Cassava bagasse, Lignocellulose nanofibers

Disciplines
Agricultural Science | Food Chemistry | Food Processing | Food Science | Human and Clinical Nutrition | Molecular, Genetic, and Biochemical Nutrition

Comments
This accepted article is published as Travalini, A.P., Lamsal, B., Magalhaes, W.L.E., Demiate, I.M. Cassave starch films reinforced iwth lignocellulose nanofibers from cassava bagasse. International Journal of Biological Macromolecules. (October 15, 2019) 139; 1151-1161. Doi: 10.1016/j.ijbiomac.2019.08.115. Posted with permission.

Cassava starch films reinforced with lignocellulose nanofibers from cassava bagasse

Ana Paula Travalini[1, 2], Buddhi Lamsal[1]*, Washington Luiz Esteves Magalhães[3], Ivo Mottin Demiate[2]*

[1]Department of Food Science and Human Nutrition, Iowa State University, Ames, IA 50011, USA

[2]Department of Food Engineering, Ponta Grossa State University, Ponta Grossa, PR, 84030900, Brazil

[3]Empresa Brasileira de Pesquisa Agropecuária, Centro Nacional de Pesquisa de Florestas. Estrada da Ribeira, km 111, Guaraituba 83411000 - Colombo, PR, Brazil – P.O. box 319

*Corresponding authors: lamsal@iastate.edu (B. Lamsal); demiate@uepg.br (I. Demiate)

Abstract

Cassava bagasse, a high-fiber coproduct of cassava starch processing, was used to produce lignocellulose nanofibers (LCNF) to apply as reinforcement in cassava starch films. LCNF-reinforced cast starch films were evaluated for changes in structural, thermal and mechanical properties and compared with control films reinforced with commercial grade nanoclay (Nclay). Five different types of cassava starch cast-films were produced: no-reinforcement control, two LCNF-reinforced, and two Nclay-reinforced, each at 0.65 and 1.3% w w^{-1}. The LCNF morphology showed the characteristic microscopic structure of lignocellulose nanofibers, with an aspect ratio > 85 and average diameter of 4.5 nm. All reinforced films were translucent and had a good distribution of the nanoparticles within. The opacity values reduced for the films with all nanoreinforcements, compared to control. The permeability to water vapor reduced with reinforcements, with lower values for the films tested with LCNF 0.65 and

Nclay 1.3. Thermal stability improved with 1.3% of LCNF and both concentrations of Nclay. Tensile stress for films increased and elongation at break value decreased with both types of nanoreinforcements.

Keywords: Starch; cassava bagasse; lignocellulose nanofibers.

Highlights

- Films reinforced with LCNF performed better compared with films with Nclay.
- The elongation at break decreased and the tensile stress increased with both reinforcements.
- The films can be applied as food packaging due to barrier and tensile properties.

37 **Graphical abstract**

38

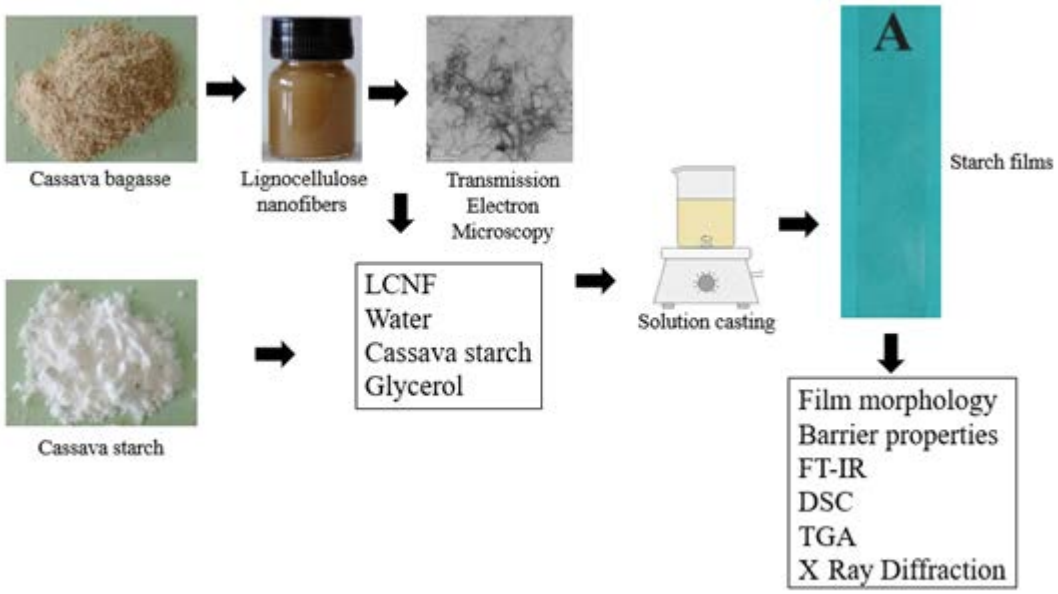

39

40

1. Introduction

Conventional food packaging raw materials are produced from non-renewable resources like petroleum, which are harmful to environment, prompting the need for investigating alternative resources [1]. Biodegradable alternatives would help to change the current situation [2]. Increasing environmental pollution has encouraged researchers to develop biodegradable/edible films and coatings, which, however, represent only 5-10% of the current plastics market due to higher costs [3]. Biodegradable agroindustry wastes, including sugarcane bagasse, cassava bagasse, and malt bagasse [4], as well as starches, can be utilized in manufacturing or reinforcing films for packaging purposes.

Cassava (*Manihot esculenta* C.), a root crop widely cultivated in tropical countries, is rich in starch. The industrial production of cassava starch involves separation of starch and fibers, resulting in a purified starch and fibrous solid residue, named cassava bagasse [5]. Cassava starch is an ingredient with excellent functional characteristics, exploited in formulation of many foods and biodegradable materials [6]. However, films made from starch are fragile, with poor mechanical properties, and more hydrophilic in nature [7,8], which limit their application in packaging of high-moisture foods and products. The addition of fillers, for example, fibers from cassava bagasse, can improve some of the desired properties of resulting films [9] and composites. Cassava bagasse has residual starch, fibers, with 38% cellulose and 37% hemicellulose, and lignin [10]. It is a low-value material that can be useful in various higher-value applications, such as production of organic acids, biodegradable packaging, nanoparticles, nanofibers, ethanol, biofuel, lactic acid, α-amylase, and others [11].

Cassava bagasse nanofibers can be prepared by mechanical treatment, resulting in a nanosized range from 1-100 nm in one dimension and applied as reinforcement in biopolymer films to improve mechanical, thermal, and barrier properties [12]. Cellulose

nanofibril is a term used for fibrils with a diameter between 3 and 15 nm and a length between 0.5 and 2 µm [13]. Lignocellulose nanofibers (LCNF) from cassava bagasse fiber has the advantage of being biodegradable, non-toxic, widely available, and resistant [14], and can be produced using a combination of mechanical, chemical, and enzymatic pretreatments [15,16].

Few studies were published considering the reinforcement of cassava starch film with lignocellulose nanofibers from raw cassava bagasse (containing > 80% starch). The goal of this study was to produce for the first time LCNF from fibrous starch-free cassava bagasse and evaluate the effect of incorporation of LCNF in cassava starch films. The chemical and technological characteristics of reinforced cassava starch films were evaluated and compared with commercial nanomaterial reinforcement (nanoclay).

2. Materials and Methods

2.1. Materials

Cassava bagasse (27% cellulose, 30% hemicellulose and 2.7% lignin) and cassava starch with an amylose content of 25% were provided by Nutriamidos (Amaporã, Brazil). We have enzymatically treated the cassava bagasse with α-amylase (Termamyl®, 0.5 g of enzyme preparation/kg starch, Novozymes, Araucária, Brazil) and amyloglucosidase (AMG®, 1.13 g of enzyme preparation/kg starch, Novozymes, Araucária, Brazil) in the laboratory for cassava lignocellulosic nanofiber LCNF preparation, following Zimmermann, Bordeanu and Strub [17]. Cassava fiber (50 g) was suspended in distilled water (2,000 mL) and passed 20 times through a colloidal mill (Supermass Colloider Masuko Sangyo, Kawaguchi, Japan) resulting in a viscous suspension. Nanoclay (Nclay), a hydrophilic bentonite (Sigma-Aldrich, St. Louis, USA), was a suspension at 3% w w^{-1} [1] and LCNF suspension had 2.72% w w^{-1} of dry material. Commercial glycerol (Fisher Scientific, Merelbeke, Belgium) and cassava

starch were used for producing the films. LCNF suspension was used in two concentrations (0.65% and 1.3%, w w^{-1}) using glycerol as plasticizer and compared with nanoclay suspension (0.65% and 1.3%, w w^{-1}). All the chemicals were of analytical grade.

2.2. Nanomaterials Characterization

2.2.1. Zeta Potential

The zeta potential and particle size distribution for the LCNF suspensions were analyzed using the Zetasizer Nano equipment (ZS90, Malvern Instruments, Worcestershire, UK). The samples were diluted in distilled water at a proportion of 1:100 (v v^{-1}) for the zeta potential analysis.

2.2.2. Transmission Electron Microscopy (TEM)

The morphology of the LCNF and Nclay was examined by transmission electron microscopy model JEM 2100 (JEOL, Peabody, USA). Images were taken at 200 kV accelerating voltage. The diluted suspension was mixed at the same proportion with a 2% (w v^{-1}) uranyl acetate solution. A drop of diluted aqueous suspensions was deposited on the carbon-coated grids and allowed to dry at room temperature.

2.2.3. X Ray Diffraction

The X ray diffraction of LCNF and Nclay powder was performed using the Rigaku Ultima IV X ray diffractometer (Rigaku Co., Tokyo, Japan) with Cu–Kα radiation (λ = 1.5418 Å). The conditions of analysis were a voltage of 40 kV, current of 44 mA, scanning range 5–50°, and scan rate of 1° min^{-1}. Based on the XRD patterns, the overall crystallinity was determined using the Ruland method [18,19], as shown in Equation 1:

$$X_c = \frac{\sum A_{cryst}}{\sum A_{cryst} + \sum A_{amorp}} \quad (1)$$

where, A_{cryst} is the crystal region and A_{amorp} is the amorphous region.

116 2.3. Reinforced Films and their Characterization

117 2.3.1. Solvent Casting of Starch Films

118 The films were prepared according to the method proposed by Aila-Suárez et al. [20]
119 and Terrazas-Hernandez et al. [21] with some modifications, with 4% cassava starch (w
120 w^{-1}, dry basis), 2% glycerol (w w^{-1}), 0.65 or 1.3% (w w^{-1}) of LCNF/Nclay suspension.
121 The suspension with starch, glycerol, and 100 g of water was placed in a small flask
122 (300 mL) and stirred at 500 rpm for 10 min. The suspension was heated to 90°C for 10
123 min. LCNF/Nclay and 70 g of water were placed in another flask and stirred at 500 rpm.
124 After cooling the first suspension to 40°C, the suspensions were blended, magnetically
125 stirred for 5 min and centrifuged (10,000 rpm for 5 min) to remove bubbles. The
126 suspensions were poured into leveled glass plates (20 x 25.5 cm) and oven dried at 40°C
127 for 24h. The plates were then stored for three days in a desiccator with 75% relative
128 humidity (saturated NaCl solution), to allow the removal of the films from the plates.

129 2.3.2. Thickness and Density

130 The film thickness was measured by a digital micrometer (Marathon CO030150,
131 Richmond Hill, Canada), according to the ASTM method F2251 [22], considering the
132 average of eight measurements in random positions for each film. The films density (g
133 cm^{-3}) was determined from the specimen weight and volume. The specimen volume was
134 calculated from specimen area (20 mm x 20 mm) and thickness. The results were
135 obtained by average of five determinations [23].

136 2.3.3. Opacity and Moisture Content

137 A UV-visible spectrophotometer (Shimadzu UV-160, Kyoto, Japan) was used to
138 measure the films opacity according to Garrido, Etxabide, Guerrero and de la Caba [24].
139 A rectangular specimen (10.0 x 3.5 mm) was placed in the spectrophotometer cell and
140 absorbance was measured at 600 nm. The opacity value was obtained by division

between absorbance (A_{600}) and thickness (mm). Moisture content (ASTM, D644) was determined by weighing the films (w1) after they have been stocked in a chamber (43% RH, 24h), dried in an oven (105°C/24h) and weighed again (w2). The moisture content (%) was calculated according to Equation [25]:

$$MC\ (\%) = \frac{w1-w2}{w1} \times 100 \qquad (2)$$

2.3.4. Water Absorption and Solubility

Water absorption was determined according to ASTM D570 [26]. Films were dried in an oven (50°C/24h), cooled and immediately weighed (wi). The films were immersed in water at room temperature, paper-dried and weighed (wf). The water absorption (%) was calculated according to Equation 3:

$$WA\ (\%) = \frac{wf-wi}{wi} \times 100 \qquad (3)$$

Film solubility was evaluated with a dry film sample (20 x 20 mm) that was weighed and soaked in 25 mL distilled water in a beaker [27]. The beaker was placed in a water bath at 37°C for 24h. The solubility (%) of the film was calculated using the following equation (4):

$$Solubility\ (\%) = \frac{W1-W2}{W1} \times 100 \qquad (4)$$

Where *W1* is the mass of the film (g) and *W2* is the mass of residue after solubilization (g).

2.3.5. Water Vapor Permeability (WVP)

The water vapor transmission rate (WVTR) is the steady water vapor flow in unit time through unit area of a body, between two specific parallel surfaces, under specific conditions of temperature and humidity at each surface with results in grams per square meter per 24h. WVTR (Equation 5) was evaluated according to the standard ASTM D1653 [28]. In this study, the test cup (Elcometer 5100, Payne permeability cup, Argenteau, Belgium) was filled with desiccant (calcium sulfate) to produce 0% RH and

covered with the film sample (49 mm diameter). The test cup was placed in a chamber (DryKeeper, Sanplatec Corp, Osaka, Japan) at 23°C and 50% RH. The cup was weighed and the weight gained by desiccant was verified for five days, obtaining the water vapor permeability (WVP, g mm m^{-2} day^{-1} kPa^{-1}). The WVP was calculated following the Equation 6.

$$WVTR = \frac{m}{t \times A} \quad (5)$$

$$WVP = \frac{WVTR \times L}{\Delta p} \quad (6)$$

Where WVTR is expressed by g m^{-2} day^{-1}, *m* is weight (g), *t* is time (day), *L* is the film thickness (mm), *A* is test area (m^2) and Δp is the water vapor partial pressure difference across the films (kPa).

2.3.6. Fourier Transform Infrared Spectroscopy – Attenuated Total Reflectance (FT-IR/ATR) and Scanning Electron Microscopy (SEM)

The FT-IR spectra of the films were recorded using a FT-IR Spectrometer (Tensor 37, Bruker, Billerica, USA). Spectra were analyzed using Opus 7.2.139 software (Bruker, Billerica, USA). Films were then placed onto a zinc selenide crystal, and the analysis was performed within the 4,000-650 cm^{-1} region with 16 scans recorded at 2 cm^{-1} resolution. The films were assessed using a scanning electron microscope (SU4800, Hitachi Ltd., Tokyo, Japan) to image their surfaces. After gold coating (Cressington 208 HR, Watford, England), the samples were observed using an accelerating voltage of 1 kV.

2.3.7. X Ray Diffraction

The X ray diffraction of cassava starch film and films incorporated with LCNF and Nclay was performed using the Rigaku Ultima IV X ray diffractometer (Rigaku Co.,

Tokyo, Japan). The conditions of analysis were a voltage of 40 kV, current of 44 mA, scanning range 5–50°, and scan rate of 1° min-1.

2.3.8. Differential Scanning Calorimetry (DSC) and Thermogravimetric Analysis (TGA)

The thermal behavior of the films was studied by differential scanning calorimetry (TA Instruments, Q1000, New Castle, USA). Approximately 5–10 mg of the dry film sample was placed in DSC pans that were sealed. All measurements were performed at a heating rate of 10°C min^{-1} from 30°C to 280°C under a nitrogen atmosphere (50 mL min^{-1}). Thermograms were evaluated using TRIOS program (TA Instruments, New Castle, USA). The thermogravimetric analysis (TGA) was performed with a TGA Q5000 (TA Instruments, USA) for all starch films. The sample (5-10 mg) was heated from room temperature to 700°C under nitrogen atmosphere and 20°C min^{-1} heating rate.

2.3.9. Tensile Tests

The mechanical properties of the cassava starch films were determined using the ASTM-D882 standard [29]. The conditioning of the films was performed at 23°C and 40% RH for 48h before the test. Films were cut into 250 mm x 10 mm strips and then characterized using a tensile machine INSTRON 4502 (Instru-Met Corporation, New Jersey, USA) with a film grip instrument. An initial grip separation and crosshead speeds of 127 mm and 25 mm min^{-1} were used, respectively. At least five replicates were carried out for each sample.

2.3.10. Statistical Analysis

Statistical analyses consisted of analysis of variance (ANOVA) using Statistica 8.0 software (Statsoft, Tulsa, OK, USA). Tukey test ($p < 0.05$) was done to identify statistical differences between average values.

3. Results and discussion

3.1. Characteristics of Nanomaterials

In the present study, LCNF was compared with Nclay due to several previous studies developed with nanoclay because it is a commercial nanometric particle [1,30]. The zeta potential of LCNF in suspension (2.72%, w w^{-1}) was -6.47 mV and that of Nclay suspension was -2.27 mV; zeta potential quantifies the surface charges with implications for the stability of colloidal suspensions. The zeta potential value below 25 mV for LCNF and Nclay indicated that they were prone to flocculation and sedimentation, thus unstable in suspension. The zeta potential results showed that Nclay has lower suspension stability than LCNF due to the lower absolute value.

Mechanical treatment of cassava bagasse during LCNF preparation resulted in defibrillation of the cellulose fibers in cell walls, which tended to aggregate. Figure 1 shows the TEM morphology of LCNF and Nclay at nanoscale dimension. The dimensions of LCNF and Nclay suspensions were examined by TEM and dimensions were analyzed using ImageJ software (Softonic, Barcelona, Spain). The aspect ratio (AR) of LCNF was >85 and <10 for Nclay, and the mean diameter (D) was 4.5±1.6 and 12.3±2.6 (nanometer range), respectively, for LCNF and Nclay. The aspect ratio (length/diameter) is determinant in the capacity of use the lignocellulose nanofibers as reinforcement. In this case, the LCNF has greater capacity to act as reinforcement in composites or films [31,32]. This morphology information obtained is consistent with nanofibers from other sources, as rice straw [14,33].

Figure 2 shows the X ray diffraction patterns for LCNF and Nclay. The X ray diffractions of LCNF exhibited peaks around 17°, 20°, 24.5° and 28.5°, while Nclay showed peaks around 7°, 17°, 20°, 22° and 35°. Kaushik, Singh and Verma [34] studied LCNF from wheat straw and found similar peaks as cassava bagasse LCNF, while

Teixeira et al. [5] worked with LCNF from cassava bagasse and verified the same behavior.

The overall crystallinity was calculated according to Ruland Method, and found to be 31.4% and 64.5%, for LCNF and Nclay, respectively. These values indicate that Nclay has higher crystallinity when compared to LCNF, due to the low crystallinity of original cassava bagasse fiber because of the presence of hemicellulose and lignin [35].

3.2. Cassava Starch Films Characterization

3.2.1. Physical Characteristics and Appearance

Film suspensions required centrifugation for bubble removal (Figure 3) prior to casting and drying. The drying temperature and the relative humidity should be controlled during film casting and storage to control film properties such as thickness, permeability and mechanical characteristics [36]. The thickness, density and opacity of cassava starch films reinforced with LCNF and Nclay are shown in Table 1. The thicknesses of all films were between 0.11 and 0.13 mm. The films reinforced with nanoparticles presented higher density when compared to films without incorporation; films reinforced with LCNF showed higher density than those incorporated with Nclay. According to the opacity values, the films presented similar translucent, except for the film incorporating 0.65% LCFL. These films had less opacity compared with films from other similar studies; for example, Kim, Jane and Lamsal [37] with values between 1.26 and 2.04 A_{600} mm^{-1}, and Nawab et al. [27] with values between 2.75 and 4.89 A_{600} mm^{-1}.

The moisture content, water absorption, solubility and water vapor permeability of cassava starch films reinforced with LCNF and Nclay are shown in Table 2. Moisture content was not significantly affected by nanoclay, nevertheless, was affect by LCNF addition in both concentrations. The water absorption for starch films decreased with

presence of LCNF and Nclay, but the films with LCNF resulted in lower values if compared with the films with Nclay. The lowest value was found for films with 1.3% LCNF (42.15%), resulting in a reduction of 62% in water absorption, followed by LCNF 0.65% with 47.55% of reduction.

The solubility of the starch films decreased with the incorporation of the nanoparticles. Starch films with LCNF showed higher solubility than those with Nclay, due to the presence of hydroxyl groups from LCNF, increasing the affinity with water, resulting in greater solubility in water [38]. In addition, the solubility of starch films is increased with the increase in the plasticizer content; therefore, glycerol increased the solubility of the films [39]. The solubility of the films is an important parameter because it indicates their integrity in aqueous media; films with higher water resistance will have a lower solubility value [40]. Water solubility is a crucial parameter in defining the applications for biopolymer composite films [41]. Certain applications, as food packaging, may require low water solubility to maintain product integrity whilst other applications such as in encapsulation, candy wrap etc., may require significantly higher solubility.

3.2.2. Film Barrier Properties

The water vapor permeability of all films is presented in Table 2. A reduction in WVP values was observed with LCNF and Nclay addition, at both 0.65 and 1.3% levels, respectively. However, a lower value (0.032 g mm m^{-2} day^{-1} kPa^{-1}) was obtained for LCNF with lower concentration, while the highest value was observed for LCNF with a higher concentration (0.047 g mm m^{-2} day^{-1} kPa^{-1}). In this case, the lower concentration of LCNF from cassava fiber presents a lower value if compared with a commercial nanoparticle, indicating that incorporation of 0.65% LCNF improves the barrier properties of cassava starch films.

The reduction in permeability is strongly associated with a decrease in diffusion coefficient imposed by the presence of nanoparticles [34]. The LCNF particles act as barrier for water vapor, thus decreasing water vapor transmission rate through the starch matrix and LCNF films. This phenomenon can be explained by the addition of LCNF that presents a tortuous path for the water molecules to pass through [41]. The highest weight gain by desiccators in beakers occurred on the first day of exposure to high humidity and remained constant on subsequent days. Guimarães et al. [42] also reported decreased WVP of starch films with incorporation of microfibrillated cellulose from carrots.

3.2.3. Structural and Morphology Properties

Figure 4 presents the FT-IR spectra for reinforced cassava starch films employed to evaluate the molecular interactions between the components. The peak at 3,304 cm^{-1} occurred due to the elongation of the O-H group present in the starch [43]. The band present in 2,927 cm^{-1} represents the C-H group, indicating the presence of glycerol [44]. The peaks found in 1,645 and 1,454 cm^{-1} refer to the water vibration present in the films and the $C-H_2$ flexion, respectively [45,46]. The band at 1,336 cm^{-1} represents the C-H vibrations, whereas in 1,240 cm^{-1} the C-O stretch of the C-O-C bond is obtained [47]. At 1,150 cm^{-1} the C-O stretch present in the C-O-H group in cassava starch was observed [46]. The bands at 925 and 760 cm^{-1} occurred due to the C-O and C-O-C stretching of glucose in starch, respectively [7,47]. The bands are characteristic of starch films without nanoparticles, which is due to the low concentration of LCNF and Nclay in their compositions.

The surface morphology of starch films with (Figure 5 b, c, d and e) and without (Figure 5a) reinforcements was investigated by SEM. The micrographs show homogeneous surface of the films containing nanoreinforcements. All the films

315 produced had a homogeneous surface with no bubbles or cracks, and good handling
316 characteristics. The films displayed a rather uniform surface but contain some hard
317 particles that have left voids in their surfaces. These hard particles could be small starch
318 gel lumps and their presence associated with voids creates a significant number of
319 flaws, which can lead to low ductility. The nanofibers are well dispersed and covered by
320 the matrix. The same behavior was reported by Kaushik et al. [34] with cellulose
321 nanofibril from wheat straw in thermoplastic starch and by Souza et al. [48] that studied
322 cassava starch films.
323 The wide-angle X ray diffraction patterns of cassava starch film (CS) and cassava starch
324 films reinforced with 0.65% and 1.3% of LCNF and Nclay are shown in Figure 6. The
325 CS, LCNF 0.65, LCNF 1.3 and Nclay 0.65 exhibited diffraction peaks at $2\theta = 5.5°$, 17°,
326 20° and 22°. Nclay 1.3, however, showed diffraction peaks at 17° and 20°. The A-type
327 structure is found in normal cereal starches and B-type structure is common in tuber and
328 high-amylose cereal starches. The CS presents a C-type crystalline structure due the
329 peaks that indicate a mixture of A- and B-type crystals structures [49]. The diffraction
330 peaks were supported by other studies with starch films [27,50]. The intensity of those
331 peaks increased with incorporation of 0.65% LCNF in cassava starch, suggesting its
332 presence in their particular concentration levels, also suggesting increased crystallinity,
333 induced due to better interaction between CS and LCNF. The intensity of peaks with
334 LCNF 1.3 and Nclay 1.3 also increased, but at a lower level in relation to LCNF 0.65.
335 3.2.4. Thermal and Mechanical Properties
336 Thermal stability of the cassava starch films was determined using DSC. Table 3
337 presents the transition temperatures (To, Tp, Tc) and enthalpy values. In the Figure 7
338 are showed the DSC curves of the pure cassava starch film and the cassava starch films
339 with LCNF and Nclay.

Pure cassava starch film had an endothermic peak at 250.5°C, but this value decreases with the addition of LCNF (240.4 and 233.4°C) and Nclay (228.6 and 226.3°C), referring to glycerol volatilization [51]. This behavior could be explained because DSC analysis was performed in sealed aluminium crucibles up to 280ºC and possibly there was moisture leaking. Studies of thermal properties of starch by DSC with sealed aluminium crucibles are scarce and the higher reported temperature is 220ºC [52]. Affinity for water is different among the film formulations and water retention inside the crucibles would be distinct. Liu et al. [52] studied *in situ* thermal decomposition of starch with constant moisture in a sealed system. Those authors reported a reduction in decomposition exotherms with increasing moisture inside the crucibles.

The peaks for glycerol volatilization are so large that the other phase transition peaks such as melting, crystallization and gelatinization cannot be assessed. Peaks at similar temperatures were observed in corn starch studies [52, 53, 54]. The DSC curves (Figure 7) indicated that the pure cassava starch film and the cassava starch films with LCNF and Nclay show a similar trend in the heating process with increasing temperature.

The nanomaterial reinforcements had some influence on the enthalpy (ΔHm) of the cassava starch films. The presence of both LCNF and Nclay resulted in higher enthalpy values. The ΔHm of pure cassava starch film was 46.5 J g^{-1}, which increased to 58.5 J g^{-1} after adding 0.65% LCNF, and to 60.8 J g^{-1} after adding 1.3% LCNF. Adding 0.65% Nclay, the ΔHm increased to 69.7 J g^{-1}, whereas adding 1.3% Nclay the ΔHm increased to 70.58 J g^{-1}. Similar pattern was reported by Savadekar and Mhaske [55] with addition of nanocellulose fibers in thermoplastic starch, and by Kaushik et al. [34] with wheat straw nanofibril.

Thermal degradation of films by DTA curves (Figure 8) indicated three peaks for each type of film. The onset decomposition temperature, peaks, and percentage of residues at

200°C, 400°C and 600°C of the cassava starch films are shown in Table 4. An initial loss of weight was observed at temperatures between 124.5 and 136.5°C, which corresponds to the elimination of the water and low molar weight compounds present in the sample by dehydration [56]. After this first stage, a decomposition step, observed at around 320°C, was attributed to starch and glycerol decomposition, due the elimination of hydroxyl groups, decomposition and depolymerization of the starch carbon chains. In this stage occurs the highest thermal degradation rate (~70%) which is reflected by the drastic weight reduction of films. The last stage corresponds to the carbon burning. The first decomposition temperature shown in Table 4 (DTA peaks) indicated that Nclay increased the thermal stability, but the second and third temperatures of films decomposition were similar. As expected, the mass residue at 600°C increased with the addition and concentration of Nclay (0.35 and 0.76%), due the high thermal stability of nanoclay, like other inorganic matrices [57].

Physical properties (tensile stress) in packaging materials are important in assessing the packaging ability to protect against external factors, in addition to reducing the deterioration rates of packaged food [58]. Table 5 shows the results of tensile tests of LCNF and Nclay-reinforced cassava starch films. An increase in tensile stress for all films was observed compared with cassava starch sample (4.8 MPa), with the highest value for LCNF 1.3 sample (6.6 MPa) (37.5% improvement), indicating good intermolecular interaction between cassava starch and LCNF. The different behavior was showed for elongation at break ($p < 0.05$), where LCNF 1.3 (44.43%) and Nclay 1.3 (43.78%) presented lower values compared with CS (54.92%), meaning that the nanoreinforcement incorporation resulted in a lower film flexibility.

Jiang et al. [41] studied properties of starch films enhanced with potato starch nanoparticles and found similar results for tensile stress and elongation at break, where

the tensile stress value increased due to the strong interaction between starch and nanoreinforcement, and elongation at break reduced due to possible agglomerated formed inside the films. The same pattern was reported by Ma et al. [44] that studied cassava starch films incorporated with cellulose nanocrystals and by Pelissari et al. [59] that worked with banana starch nanocomposites with cellulose nanofibers. Savadekar and Mhaske [55] evaluated the effect of the nanocellulose fibers (LCNF) addition on thermoplastic starch (TPS) and 0.4% LCNF improved the tensile stress (46.10%), while elongation at break decreased.

4. Conclusion

LCNF from cassava bagasse was prepared using colloidal mill, after enzyme treatment to remove residual starch. All cassava starch films were translucent, flexible, and bubble free, potentially applicable for packaging, comparable to commercial films. TEM micrographs revealed that the nanoparticles had characteristic shape of nanofibril (diameter between 3 and 15 nm and aspect ratio >85). LCNF and Nclay were used to produce cassava starch films by solution casting with cassava starch, glycerol and water. Opacity and water absorption values of films reduced significantly and tensile stress of starch films with nanoreinforcements were increased when compared to CS. The water vapor permeability value was reduced for LCNF 0.65 and Nclay 1.3, and a lower concentration of LCNF resulted in the lowest WVP value. The mechanical and barrier properties of starch films showed that lignocellulose nanofibers from cassava bagasse can be employed to reinforce starch films with potential uses in food packaging.

ACKNOWLEDGEMENT: Authors acknowledge support by CAPES (Brazil) for Ms. Travalini's exchange program at Iowa State University. Dr. Ivo Mottin Demiate is a research fellow from CNPq (Brazil). This article is also a product of the Iowa

414 Agriculture and Home Economics Experiment Station, Ames, Iowa. Project No.
415 IOW03902 is sponsored by Hatch Act and State of Iowa funds.
416

417 **References**

418 [1] C.K. Saurabh, S. Gupta, P.S. Variyar, A. Sharma, Effect of addition of nanoclay,
419 beeswax, tween-80 and glycerol on physicochemical properties of guar gum
420 films, Ind. Crops Prod. 89 (2016) 109–118.
421 [2] A.C. Souza, R. Benze, E.S. Ferrão, C. Ditchfield, A.C. V Coelho, C.C. Tadini,
422 Cassava starch biodegradable films: Influence of glycerol and clay nanoparticles
423 content on tensile and barrier properties and glass transition temperature, LWT -
424 Food Sci. Technol. 46 (2012) 110–117.
425 doi:http://dx.doi.org/10.1016/j.lwt.2011.10.018.
426 [3] C.L. Luchese, T. Garrido, J.C. Spada, I.C. Tessaro, K. de la Caba, Development
427 and characterization of cassava starch films incorporated with blueberry pomace,
428 Int. J. Biol. Macromol. 106 (2018) 834–839.
429 [4] L.R.P.F. Mello, S. Mali, Use of malt bagasse to produce biodegradable baked
430 foams made from cassava starch, Ind. Crops Prod. 55 (2014) 187–193.
431 [5] E. de M. Teixeira, D. Pasquini, A.A.S. Curvelo, E. Corradini, M.N. Belgacem, A.
432 Dufresne, Cassava bagasse cellulose nanofibrils reinforced thermoplastic cassava
433 starch, Carbohydr. Polym. 78 (2009) 422–431.
434 doi:http://dx.doi.org/10.1016/j.carbpol.2009.04.034.
435 [6] J. Colivet, R.A. Carvalho, Hydrophilicity and physicochemical properties of
436 chemically modified cassava starch films, Ind. Crops Prod. 95 (2017) 599–607.
437 doi:https://doi.org/10.1016/j.indcrop.2016.11.018.
438 [7] A. Akhavan, F. Khoylou, E. Ataeivarjovi, Preparation and characterization of

gamma irradiated Starch/PVA/ZnO nanocomposite films, Radiat. Phys. Chem. 138 (2017) 49–53.

[8] A. Dufresne, J. Castaño, Polysaccharide nanomaterial reinforced starch nanocomposites: A review, Starch – Stärke. 69 (2017) 1–19.

[9] R. Colussi, V.Z. Pinto, S.L.M. El Halal, B. Biduski, L. Prietto, D.D. Castilhos, E. da Rosa Zavareze, A.R.G. Dias, Acetylated rice starches films with different levels of amylose: Mechanical, water vapor barrier, thermal, and biodegradability properties, Food Chem. 221 (2017) 1614–1620.

[10] A. Edhirej, S.M. Sapuan, M. Jawaid, N.I. Zahari, Cassava/sugar palm fiber reinforced cassava starch hybrid composites: Physical, thermal and structural properties, Int. J. Biol. Macromol. 101 (2017) 75–83. doi:10.1016/j.ijbiomac.2017.03.045.

[11] T.C. Polachini, L.F.L. Betiol, J.F. Lopes-Filho, J. Telis-Romero, Water adsorption isotherms and thermodynamic properties of cassava bagasse, Thermochim. Acta. 632 (2016) 79–85.

[12] H. Pham, Q.P. Nguyen, Effect of silica nanoparticles on clay swelling and aqueous stability of nanoparticle dispersions, J. Nanoparticle Res. 16 (2014) 2137.

[13] D.O. Castro, Z. Karim, L. Medina, J.O. Häggström, F. Carosio, A. Svedberg, L. Wågberg, D. Söderberg, L.A. Berglund, The use of a pilot-scale continuous paper process for fire retardant cellulose-kaolinite nanocomposites, Compos. Sci. Technol. 162 (2018) 215–224. doi:https://doi.org/10.1016/j.compscitech.2018.04.032.

[14] E.A. Hassan, M.L. Hassan, Rice straw nanofibrillated cellulose films with antimicrobial properties via supramolecular route, Ind. Crops Prod. 93 (2016)

142–151.

[15] N. Kawee, N.T. Lam, P. Sukyai, Homogenous isolation of individualized bacterial nanofibrillated cellulose by high pressure homogenization, Carbohydr. Polym. 179 (2018) 394–401.

[16] W. Wang, T. Liang, H. Bai, W. Dong, X. Liu, All cellulose composites based on cellulose diacetate and nanofibrillated cellulose prepared by alkali treatment, Carbohydr. Polym. 179 (2018) 297–304.

[17] T. Zimmermann, N. Bordeanu, E. Strub, Properties of nanofibrillated cellulose from different raw materials and its reinforcement potential, Carbohydr. Polym. 79 (2010) 1086–1093. doi:http://dx.doi.org/10.1016/j.carbpol.2009.10.045.

[18] W. Ruland, X-ray determination of crystallinity and diffuse disorder scattering, Acta Crystallogr. 14 (1961) 1180–1185.

[19] C. Li, T. Jiang, J. Wang, H. Wu, S. Guo, X. Zhang, J. Li, J. Shen, R. Chen, Y. Xiong, In Situ Formation of Microfibrillar Crystalline Superstructure: Achieving High-Performance Polylactide, ACS Appl. Mater. Interfaces. 9 (2017) 25818–25829.

[20] S. Aila-Suárez, H.M. Palma-Rodríguez, A.I. Rodríguez-Hernández, J.P. Hernández-Uribe, L.A. Bello-Pérez, A. Vargas-Torres, Characterization of films made with chayote tuber and potato starches blending with cellulose nanoparticles, Carbohydr. Polym. 98 (2013) 102–107.

[21] J.A. Terrazas-Hernandez, J.D.J. Berrios, G.M. Glenn, S.H. Imam, D. Wood, L.A. Bello-Pérez, A. Vargas-Torres, Properties of Cast Films Made of Chayote (Sechium edule Sw.) Tuber Starch Reinforced with Cellulose Nanocrystals, J. Polym. Environ. 23 (2015) 30–37. doi:10.1007/s10924-014-0652-0.

[22] ASTM, American Society for Testing and Materials - F2251, in: Annu. B. ASTM

Stand., ASTM, Philadelphia, 2013.

[23] L. Ren, X. Yan, J. Zhou, J. Tong, X. Su, Influence of chitosan concentration on mechanical and barrier properties of corn starch/chitosan films, Int. J. Biol. Macromol. (2017).

[24] T. Garrido, A. Etxabide, P. Guerrero, K. de la Caba, Characterization of agar/soy protein biocomposite films: Effect of agar on the extruded pellets and compression moulded films, Carbohydr. Polym. 151 (2016) 408–416.

[25] ASTM, American Society for Testing and Materials - D644, in: Annu. B. ASTM Stand., ASTM, Philadelphia, 2002.

[26] ASTM, American Society for Testing and Materials - D570, in: Annu. B. ASTM Stand., ASTM, Philadelphia, 2010.

[27] A. Nawab, F. Alam, M.A. Haq, Z. Lutfi, A. Hasnain, Mango kernel starch-gum composite films: Physical, mechanical and barrier properties, Int. J. Biol. Macromol. 98 (2017) 869–876.

[28] ASTM, American Society for Testing and Materials - D1653, in: Annu. B. ASTM Stand., ASTM, Philadelphia, 2013.

[29] ASTM, American Society for Testing and Materials - D882, in: Annu. B. ASTM Stand., ASTM, Philadelphia, 2012.

[30] B. Biduski, J.A. Evangelho, F.T. Silva, M. El Halal, S. Lisie, A.S. Takimi, N.L.V. Carreño, A.R.G. Dias, E. Rosa Zavareze, Physicochemical properties of nanocomposite films made from sorghum oxidized starch and nanoclay, Starch äSte. (2017).

[31] J. Chandra, N. George, S.K. Narayanankutty, Isolation and characterization of cellulose nanofibrils from arecanut husk fibre, Carbohydr. Polym. 142 (2016) 158–166. doi:https://doi.org/10.1016/j.carbpol.2016.01.015.

[32] S. Deng, J. Ma, Y. Guo, F. Chen, Q. Fu, One-step modification and nanofibrillation of microfibrillated cellulose for simultaneously reinforcing and toughening of poly(ε-caprolactone), Compos. Sci. Technol. 157 (2018) 168–177. doi:https://doi.org/10.1016/j.compscitech.2017.10.029.

[33] A.M. Khalil, M.L. Hassan, A.A. Ward, Novel nanofibrillated cellulose/polyvinylpyrrolidone/silver nanoparticles films with electrical conductivity properties, Carbohydr. Polym. 157 (2017) 503–511.

[34] A. Kaushik, M. Singh, G. Verma, Green nanocomposites based on thermoplastic starch and steam exploded cellulose nanofibrils from wheat straw, Carbohydr. Polym. 82 (2010) 337–345. doi:https://doi.org/10.1016/j.carbpol.2010.04.063.

[35] A. Thygesen, J. Oddershede, H. Lilholt, A.B. Thomsen, K. Ståhl, On the determination of crystallinity and cellulose content in plant fibres, Cellulose. 12 (2005) 563.

[36] A.P. Teodoro, S. Mali, N. Romero, G.M. de Carvalho, Cassava starch films containing acetylated starch nanoparticles as reinforcement: Physical and mechanical characterization, Carbohydr. Polym. 126 (2015) 9–16. doi:https://doi.org/10.1016/j.carbpol.2015.03.021.

[37] H.-Y. Kim, J. Jane, B. Lamsal, Hydroxypropylation improves film properties of high amylose corn starch, Ind. Crops Prod. 95 (2017) 175–183. doi:https://doi.org/10.1016/j.indcrop.2016.10.025.

[38] S.L.M. El Halal, G.P. Bruni, J.A. do Evangelho, B. Biduski, F.T. Silva, A.R.G. Dias, E. da Rosa Zavareze, M. de Mello Luvielmo, The properties of potato and cassava starch films combined with cellulose fibers and/or nanoclay, Starch/Staerke. 70 (2018) 1–10. doi:10.1002/star.201700115.

[39] C.D. Poeloengasih, Y. Pranoto, S.N. Hayati, Hernawan, V.T. Rosyida, D.J.

Prasetyo, T.H. Jatmiko, W. Apriyana, A. Suwanto, A physicochemical study of sugar palm (Arenga Pinnata) starch films plasticized by glycerol and sorbitol, in: AIP Conf. Proc., AIP Publishing, 2016: p. 80003.

[40] S. Zhang, H. Zhao, Preparation and properties of zein–rutin composite nanoparticle/corn starch films, Carbohydr. Polym. 169 (2017) 385–392.

[41] S. Jiang, C. Liu, X. Wang, L. Xiong, Q. Sun, Physicochemical properties of starch nanocomposite films enhanced by self-assembled potato starch nanoparticles, LWT - Food Sci. Technol. 69 (2016) 251–257. doi:10.1016/j.lwt.2016.01.053.

[42] I.C. Guimarães, K.C. dos Reis, E.G.T. Menezes, A.C. Rodrigues, T.F. da Silva, I.R.N. de Oliveira, E.V. de B.V. Boas, Cellulose microfibrillated suspension of carrots obtained by mechanical defibrillation and their application in edible starch films, Ind. Crops Prod. 89 (2016) 285–294.

[43] A.A. AL-Hassan, M.H. Norziah, Effect of transglutaminase induced crosslinking on the properties of starch/gelatin films, Food Packag. Shelf Life. 13 (2017) 15–19.

[44] X. Ma, Y. Cheng, X. Qin, T. Guo, J. Deng, X. Liu, Hydrophilic modification of cellulose nanocrystals improves the physicochemical properties of cassava starch-based nanocomposite films, LWT - Food Sci. Technol. 86 (2017) 318–326. doi:https://doi.org/10.1016/j.lwt.2017.08.012.

[45] P. Patel, P. Agarwal, S. Kanawaria, S. Kachhwaha, S.L. Kothari, Plant-Based Synthesis of Silver Nanoparticles and Their Characterization, in: Nanotechnol. Plant Sci., Springer, 2015: pp. 271–288.

[46] J. Prachayawarakorn, S. Chaiwatyothin, S. Mueangta, A. Hanchana, Effect of jute and kapok fibers on properties of thermoplastic cassava starch composites,

564 Mater. Des. 47 (2013) 309–315.
565 [47] A. López-Córdoba, C. Medina-Jaramillo, D. Piñeros-Hernandez, S. Goyanes,
566 Cassava starch films containing rosemary nanoparticles produced by solvent
567 displacement method, Food Hydrocoll. 71 (2017) 26–34.
568 doi:http://dx.doi.org/10.1016/j.foodhyd.2017.04.028.
569 [48] A.C. Souza, G.E.O. Goto, J.A. Mainardi, A.C. V Coelho, C.C. Tadini, Cassava
570 starch composite films incorporated with cinnamon essential oil: Antimicrobial
571 activity, microstructure, mechanical and barrier properties, LWT - Food Sci.
572 Technol. 54 (2013) 346–352. doi:https://doi.org/10.1016/j.lwt.2013.06.017.
573 [49] B. Montero, M. Rico, S. Rodríguez-Llamazares, L. Barral, R. Bouza, Effect of
574 nanocellulose as a filler on biodegradable thermoplastic starch films from tuber,
575 cereal and legume, Carbohydr. Polym. 157 (2017) 1094–1104.
576 doi:10.1016/j.carbpol.2016.10.073.
577 [50] M. Guimarães Jr, V.R. Botaro, K.M. Novack, F.G. Teixeira, G.H.D. Tonoli,
578 Starch/PVA-based nanocomposites reinforced with bamboo nanofibrils, Ind.
579 Crops Prod. 70 (2015) 72–83.
580 [51] F. Chivrac, E. Pollet, M. Schmutz, L. Avérous, Starch nano-biocomposites based
581 on needle-like sepiolite clays, Carbohydr. Polym. 80 (2010) 145–153.
582 doi:https://doi.org/10.1016/j.carbpol.2009.11.004.
583 [52] X. Liu, L. Yu, H. Liu, L. Chen, L. Li, In situ thermal decomposition of starch
584 with constant moisture in a sealed system, Polym. Degrad. Stab. 93 (2008) 260–
585 262. doi:https://doi.org/10.1016/j.polymdegradstab.2007.09.004.
586 [53] A.V. Lluch, A.M. Felipe, A.R. Greus, A. Cadenato, X. Ramis, J.M. Salla, J.M.
587 Morancho, Thermal analysis characterization of the degradation of biodegradable
588 starch blends in soil, J. Appl. Polym. Sci. 96 (2005) 358–371.

doi:10.1002/app.21428.

[54] R.L. Shogren, Effect of moisture content on the melting and subsequent physical aging of cornstarch, Carbohydr. Polym. 19 (1992) 83–90. doi:https://doi.org/10.1016/0144-8617(92)90117-9.

[55] N.R. Savadekar, S.T. Mhaske, Synthesis of nano cellulose fibers and effect on thermoplastics starch based films, Carbohydr. Polym. 89 (2012) 146–151.

[56] R.M. Daudt, A.J.G. Sinrod, R.J. Avena-Bustillos, I.C. Külkamp-Guerreiro, L.D.F. Marczak, T.H. McHugh, Development of edible films based on Brazilian pine seed (*Araucaria angustifolia*) flour reinforced with husk powder, Food Hydrocoll. 71 (2017) 60–67.

[57] U. Andjelković, A. Milutinović-Nikolić, N. Jović-Jovičić, P. Banković, T. Bajt, Z. Mojović, Z. Vujčić, D. Jovanović, Efficient stabilization of Saccharomyces cerevisiae external invertase by immobilisation on modified beidellite nanoclays, Food Chem. 168 (2015) 262–269. doi:https://doi.org/10.1016/j.foodchem.2014.07.055.

[58] H.M.C. Azeredo, M.F. Rosa, L.H.C. Mattoso, Nanocellulose in bio-based food packaging applications, Ind. Crops Prod. 97 (2017) 664–671. doi:https://doi.org/10.1016/j.indcrop.2016.03.013.

[59] F.M. Pelissari, M.M. Andrade-Mahecha, P.J. do A. Sobral, F.C. Menegalli, Nanocomposites based on banana starch reinforced with cellulose nanofibers isolated from banana peels, J. Colloid Interface Sci. 505 (2017) 154–167. doi:https://doi.org/10.1016/j.jcis.2017.05.106.

614 Figures

615

616

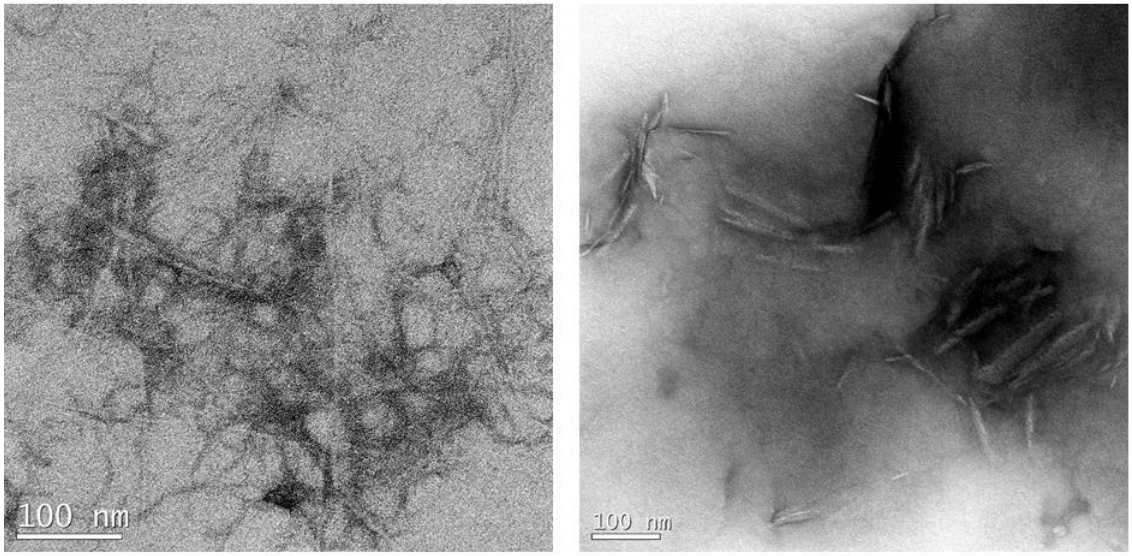

LCNF Nclay

617

618 Figure 1: TEM micrographs of LCNF and Nclay nanoparticles

619 LCNF: lignocellulose nanofibers; Nclay: nanoclay

620

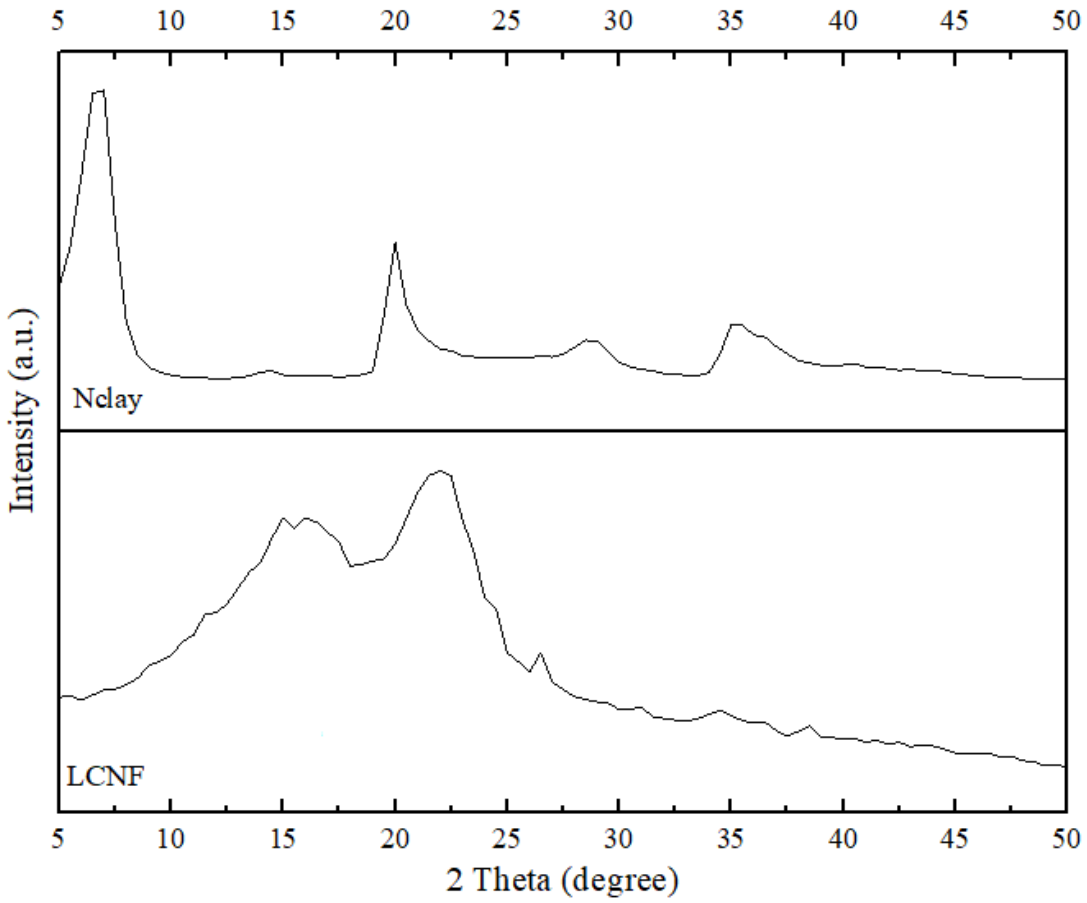

Figure 2: X ray diffractograms of LCNF and Nclay
LCNF: lignocellulose nanofibers; Nclay: nanoclay

627

628

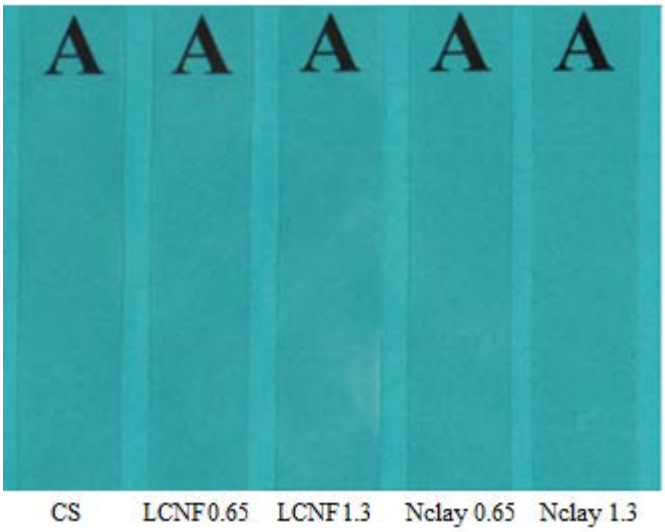

629

630 Figure 3: Typical aspect of cassava starch films without nanoparticles (CS) and with

631 LCNF and Nclay in different concentrations

632 CS: cassava starch; LCNF: lignocellulose nanofibers; Nclay: nanoclay

633

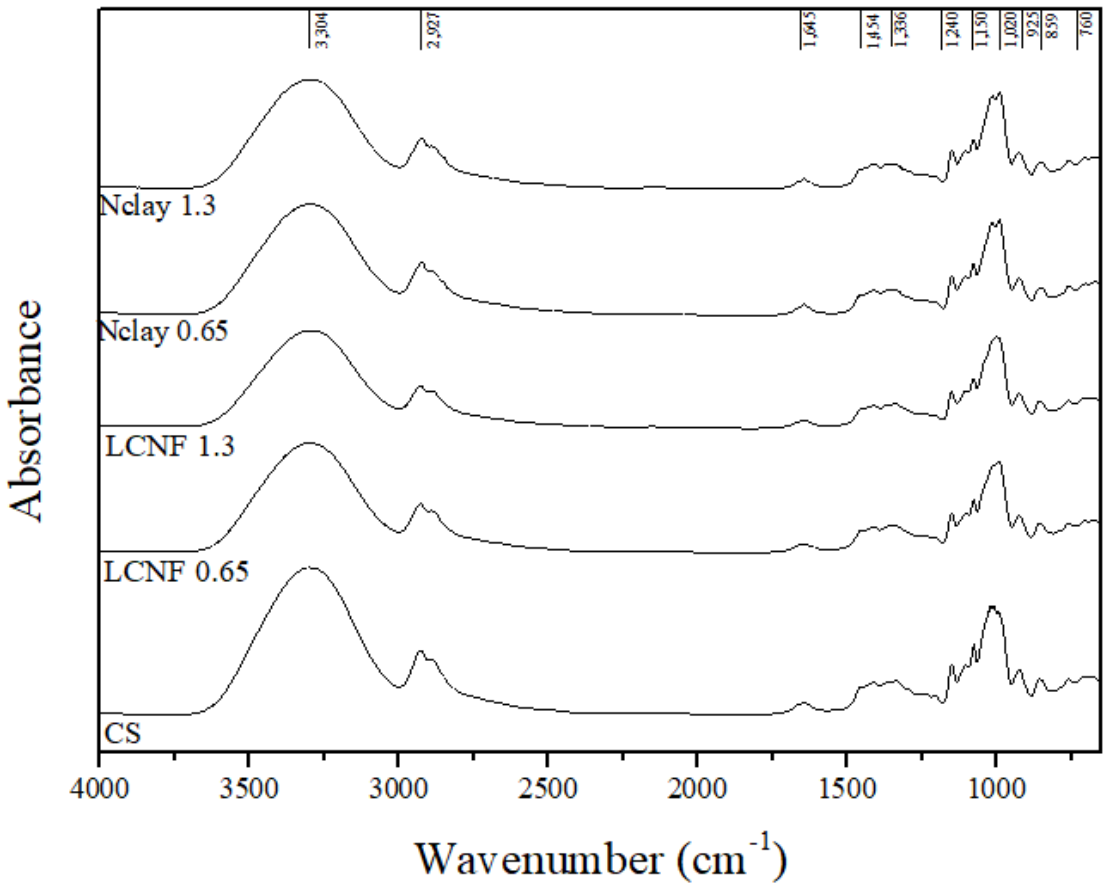

Figure 4: FT-IR absorbance spectra of cassava starch films
CS: cassava starch; LCNF: lignocellulose nanofibers; Nclay: nanoclay

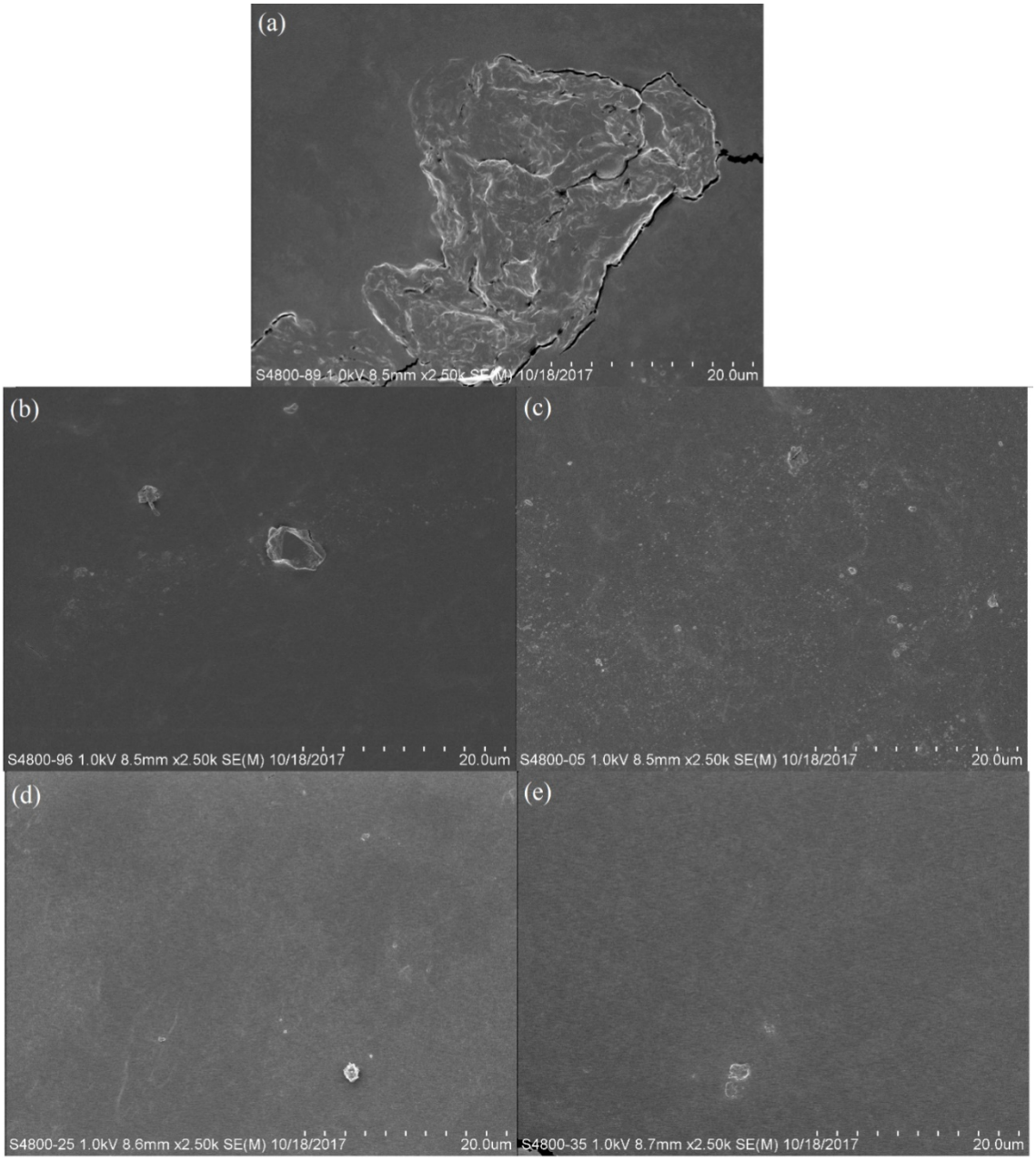

Figure 5: Films SEM (a): CS, (b): LCNF 0.65%, (c): LCNF 1.3%, (d): Nclay 0.65% and (e): Nclay 1.3% (2.5 kx)

CS: cassava starch; LCNF: lignocellulose nanofibers; Nclay: nanoclay

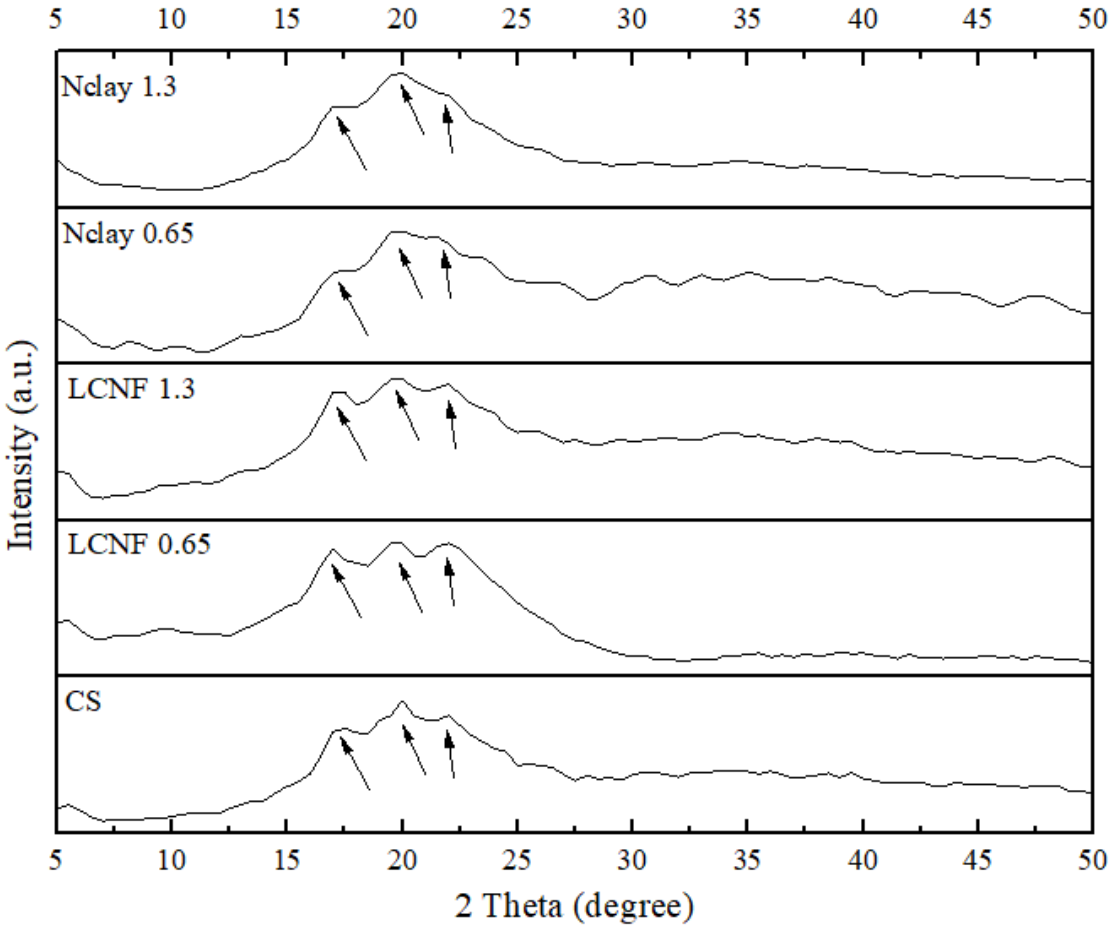

645

646 Figure 6: X ray diffractograms of CS, LCNF 0.65, LCNF 1.3, Nclay 0.65 and Nclay 1.3
647 CS: cassava starch; LCNF: lignocellulose nanofibers; Nclay: nanoclay
648

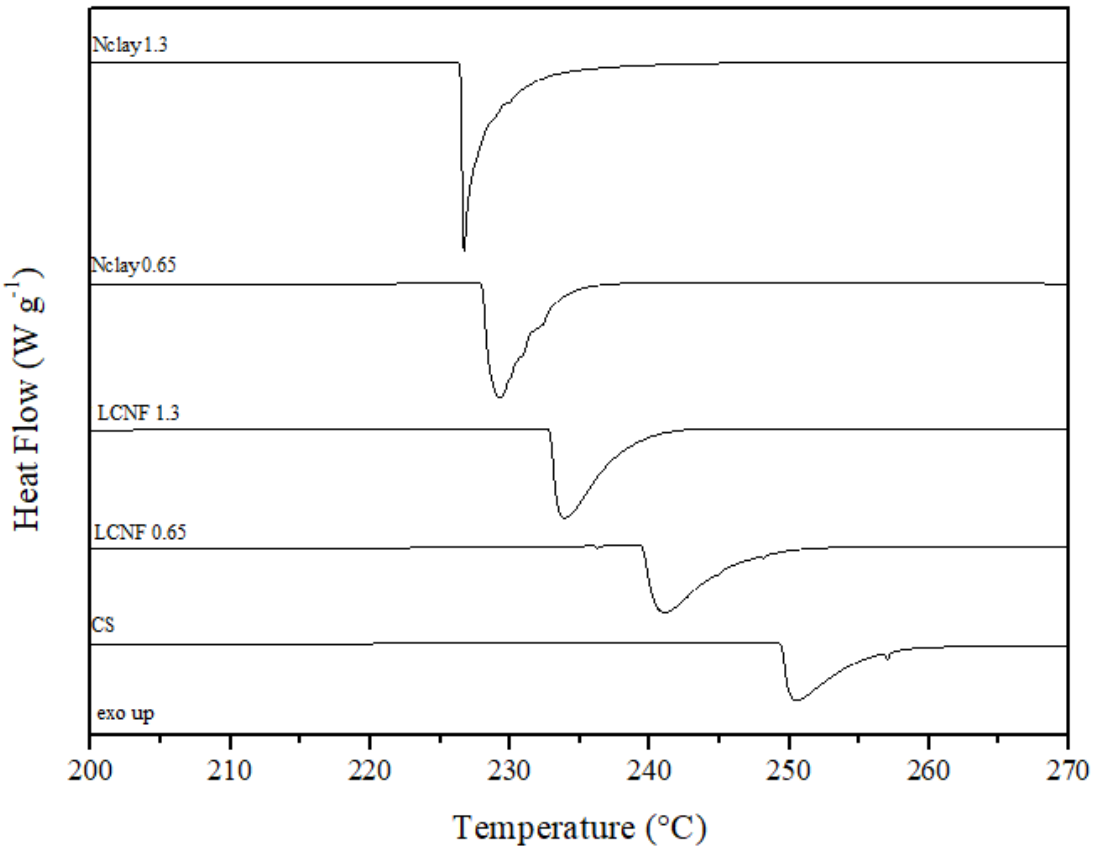

649

650 Figure 7: DSC curves of cassava starch films without nanoparticles and with LCNF
651 (0.65 and 1.3%) and Nclay (0.65 and 1.3%)
652 CS: cassava starch; LCNF: lignocellulose nanofibers; Nclay: nanoclay
653

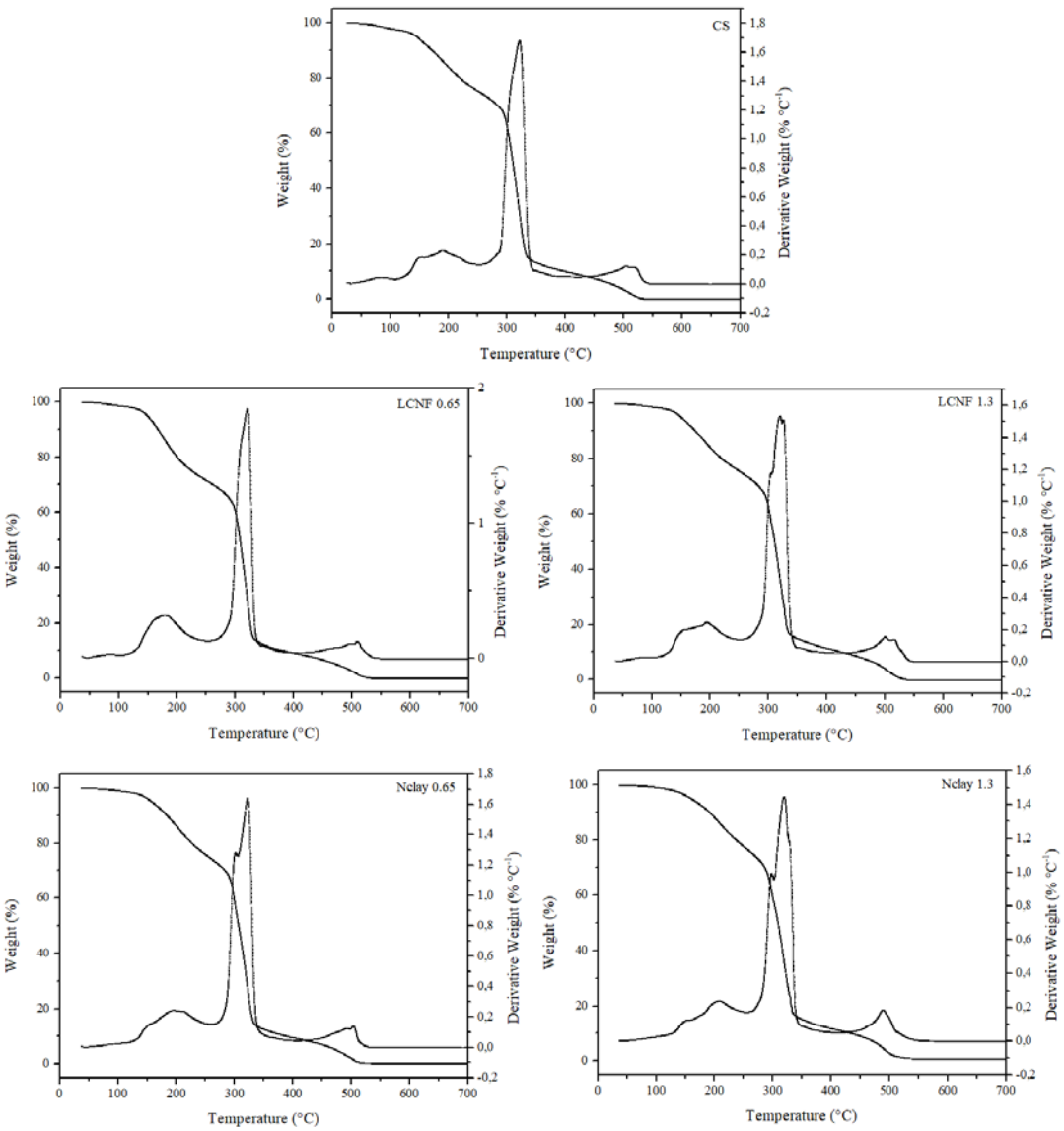

Figure 8: Thermograms (TGA and DTA curves) of cassava starch films. CS: cassava starch; LCNF: lignocellulose nanofibers; Nclay: nanoclay

667 Tables

668

669 Table 1: Average and standard deviations values of thickness, density and opacity of
670 cassava starch films

Sample	Thickness (mm)	Density (g cm^{-3})	Opacity (A_{600} mm^{-1})
CS	0.11±0.02	1.49±0.04	0.95±0.00[b]
LCNF 0.65	0.12±0.01	1.47±0.04	1.28±0.11[a]
LCNF 1.3	0.12±0.02	1.36±0.06	0.77±0.19[b]
Nclay 0.65	0.12±0.01	1.23±0.04	0.77±0.01[b]
Nclay 1.3	0.13±0.01	1.30±0.24	0.73±0.03[b]
p-ANOVA	0.43	0.27	0.01

671 * Analysis of Variance obtained by the ANOVA test.
672 ** Different letters in the same column represent statistical difference in the results according to Fisher's
673 test ($p < 0.05$).
674 CS: cassava starch; LCNF: lignocellulose nanofibers; Nclay: nanoclay.
675

676

677

678

679 Table 2: Average and standard deviations values of moisture content, water absorption,
680 solubility and water vapor permeability (WVP) of cassava starch films

Sample	Moisture Content (%)	Water Absorption (%)	Solubility (%)	WVP (g mm m^{-2} day^{-1} kPa^{-1})
CS	32.66±0.62[b]	112.48±4.79[a]	31.30±0.64[a]	0.041±0.007
LCNF 0.65	34.50±0.17[a]	47.55±0.46[c]	23.83±3.12[b]	0.032±0.001
LCNF 1.3	34.54±0.24[a]	42.15±3.18[c]	22.56±0.47[b]	0.047±0.001
Nclay 0.65	32.04±0.67[b]	49.29±0.65[c]	20.83±2.39[b]	0.045±0.002
Nclay 1.3	32.45±0.05[b]	69.55±2.88[b]	6.37±3.52[c]	0.038±0.006
p-ANOVA	<0.001	<0.0001	0.001	0.2325

681 * Analysis of Variance obtained by the ANOVA test.
682 ** Different letters in the same column represent statistical difference in the results according to Fisher's
683 test ($p < 0.05$).
684 CS: cassava starch; LCNF: lignocellulose nanofibers; Nclay: nanoclay.

685

686

687

688 Table 3: Thermal properties by DSC of cassava starch films without nanoparticles and
689 with LCNF (0.65 and 1.3%) and Nclay (0.65 and 1.3%)

	ΔH (J g^{-1})	To (°C)	Tp (°C)	Tc (°C)
CS	46.5	249.0	250.5	263.0
LCNF 0.65	58.5	238.1	240.4	256.0
LCNF 1.3	60.8	232.3	233.4	243.2
Nclay 0.65	69.7	226.5	228.6	238.3
Nclay 1.3	70.6	225.2	226.3	241.0

690 CS: cassava starch; LCNF: lignocellulose nanofibers; Nclay: nanoclay.

691

692

693

694 Table 4: Thermal properties by TGA of starch films

Sample	Onset temperature (°C)	DTA peaks (°C)			Residues (%)		
					200 °C	400 °C	600 °C
CS	124.5±0.7^{b}	189±1.4^{bc}	320.5±2.1	503.5±3.5^{a}	83.5±0.4^{c}	9.8±0.2^{b}	0.03±0.01^{c}
LCNF 0.65	134±1.4^{ab}	177.5±4.9^{c}	319.5±2.1	507.5±2.1^{a}	80.1±0.0^{d}	9.1±0.1^{c}	0.04±0.01^{c}
LCNF 1.3	130±^{ab}	196±1.4^{ab}	319±2.8	502.5±0.7^{a}	83.9±0.0^{c}	11.3±0.0^{a}	0.03±0.01^{c}
Nclay 0.65	136.5±3.5^{a}	194.5±3.5^{ab}	321.5±2.1	505.5±0.7^{a}	86.3±0.4^{b}	9.6±0.0^{bc}	0.35±0.01^{b}
Nclay 1.3	130±4.2^{ab}	206±1.4^{a}	319±1.4	486±4.2^{b}	88.1±0.2^{a}	11.8±0.2^{a}	0.76±0.01^{a}
p-ANOVA	0.03	0.001	0.74	0.003	<0.0001	<0.0001	<0.0001

695 * Analysis of Variance obtained by the ANOVA test.

696 ** Different letters in the same column represent statistical difference in the results according to Fisher's

697 test ($p < 0.05$).

698 CS: cassava starch; LCNF: lignocellulose nanofibers; Nclay: nanoclay.

699

Table 5: Values of tensile stress and elongation at break for the control film (CS) and films with LCNF and Nclay

Sample	Tensile Stress (MPa)	Elongation at Break (%)
CS	4.8±0.72[b]	54.9±2.53[a]
LCNF 0.65	5.3±0.66[ab]	48.7±2.15[ab]
LCNF 1.3	6.6±0.75[a]	44.4±3.30[b]
Nclay 0.65	5.6±0.25[ab]	47.4±1.21[b]
Nclay 1.3	4.6±0.22[b]	43.8±0.98[b]
p-ANOVA	0.01	0.001

* Analysis of Variance obtained by the ANOVA test.

** Different letters in the same column represent statistical difference in the results according to Fisher's test ($p < 0.05$).

CS: cassava starch; LCNF: lignocellulose nanofibers; Nclay: nanoclay.